Maximum Likelihood Estimation for Compound-Gaussian Clutter with Inverse Gamma Texture

The inverse gamma distributed texture is important for modeling compound-Gaussian clutter (e.g. for sea reflections), due to the simplicity of estimating its parameters. We develop maximum-likelihood (ML) and method of fractional moments (MoFM) estimates to find the parameters of this distribution. We compute the Cramér-Rao bounds (CRBs) on the estimate variances and present numerical examples. We also show examples demonstrating the applicability of our methods to real lake-clutter data. Our results illustrate that, as expected, the ML estimates are asymptotically efficient, and also that the real lake-clutter data can be very well modeled by the inverse gamma distributed texture compound-Gaussian model.

I. INTRODUCTION

Compound-Gaussian models are often used to characterize heavy-tailed clutter distributions in high-resolution radar [1, 2] as well as to model speech waveforms, fast fading channels, and various radio propagation channel disturbances (see [1] and the references therein). The key problems in compound-Gaussian clutter modeling are choosing the texture distribution and estimating its parameters. Many texture distributions have been studied (see [2]–[4] and references therein) and their parameters are typically estimated using the method of moments (MoM). We present maximum-likelihood (ML) and method of fractional moments (MoFM) estimates to find the parameters of a compound-Gaussian clutter with a texture having an inverse gamma probability density function (pdf), which leads to a closed form pdf of the clutter and simplifies the computations. Using numerical examples, we compare the mean-square errors (MSEs) of these estimates with their Cramér-Rao bounds (CRBs). We illustrate the applicability of our results to real lake-clutter data, collected by the IPIX radar of McMaster University, Hamilton, ON, Canada.

Manuscript received April 16, 2005; revised December 22, 2005 and May 4, 2006; released for publication December 16, 2006.

IEEE Log No. T-AES/43/2/903029.

Refereeing of this contribution was handled by M. Rangaswamy.

This work was supported by the Department of Defense under the Air Force Office of Scientific Research MURI Grant FA9550-05-1-0443, DARPA through the Navy Research Laboratory Grant N00173-06-1-G006, and AFOSR Grant FA9550-05-0018.

This work was developed while Alessio Balleri was visiting Prof. Nehorai's research group at the Dept. of Electrical and Computer Engineering, University of Illinois at Chicago.

II. MEASUREMENT MODEL

We present the compound-Gaussian model for a radar sea clutter. In this model, the clutter $e(t)$, where t is a discrete time index, is sampled from a given range cell at repetition frequency. It is assumed to be the product of two components [5]–[6]:

$$e(t) = \sqrt{\tau(t)} \cdot x(t), \qquad t = 1,2,3,\ldots \tag{1}$$

where the factor $x(t) = x_{\mathrm{I}}(t) + jx_{\mathrm{Q}}(t)$ is a stationary complex Gaussian process, called the speckle, which accounts for local backscattering; here $x_{\mathrm{I}}(t)$ and $x_{\mathrm{Q}}(t)$ are the in-phase (I) and quadrature (Q) components of $x(t)$, respectively. They satisfy $\mathrm{E}\{x_{\mathrm{I}}(t)\} = \mathrm{E}\{x_{\mathrm{Q}}(t)\} = 0$, with $\mathrm{E}\{x_{\mathrm{I}}(t)^2\} = \mathrm{E}\{x_{\mathrm{Q}}(t)^2\} = 1/2$ and thus $\mathrm{E}\{|x(t)|^2\} = 1$. Assume also $\mathrm{E}\{x_{\mathrm{I}}(t)x_{\mathrm{Q}}(t)\} = 0$. The factor $\tau(t)$ is a nonnegative real random process, usually called the texture; it describes the variations of the local reflected power due to the tilting of the illuminated area.

In the work presented here, we consider the inverse gamma texture distribution [7, Sect. 3.3.3], [8], in which $1/\tau(t)$ follows a gamma distribution. Hence the pdf of τ can be written as [6]–[8]

$$f_\tau(\tau;\alpha,\beta) = \frac{1}{\beta^\alpha \Gamma(\alpha)} \tau^{-(\alpha+1)} e^{-1/\beta\tau} \tag{2}$$

where α is the shape parameter, β is the scale parameter, and $\Gamma(\cdot)$ is the Gamma function. Note that in this case, the compound-Gaussian model (1) leads to a complex multivariate t distribution model for the clutter [6, 8].

Our measurement is the magnitude of the clutter, denoted by R:

$$R = |e| = \sqrt{\tau} \cdot |x| \tag{3}$$

where we omitted the index t for simplicity.

III. GENERAL RESULTS

In this section, we first derive the pdf of the measurement, namely the magnitude of the clutter. Based on this pdf, we estimate the clutter parameters with both the MoFM and ML estimators. We also compute the CRB of the clutter distribution parameter α and β.

A. PDF of Measurement Magnitude

From the measurement model (3), we derive the pdf of the magnitude using

$$f_R(r) = \int_{-\infty}^{\infty} f(r \mid \tau) f(\tau) d\tau \tag{4}$$

where r denotes a realization of the random process R. Since the texture $\tau(t)$ follows an inverse gamma distribution and the magnitude of the speckle has a Rayleigh[1] distribution [5], the pdf of the clutter magnitude is given by

$$f_R(r) = \int_0^\infty \frac{1}{\beta^\alpha \Gamma(\alpha)} \tau^{-(\alpha+1)} e^{-1/\beta\tau} \frac{2r}{\tau} e^{-r^2/\tau} d\tau$$
$$= \frac{2r}{\beta^\alpha \Gamma(\alpha)} \int_0^\infty \tau^{-(\alpha+2)} e^{-\beta r^2 + 1/\beta\tau} d\tau. \quad (5)$$

Using the change-of-variables $x = (\beta r^2 + 1)/\beta\tau$, the pdf of the clutter magnitude can be expressed as

$$f_R(r) = \frac{2r\beta}{(\beta r^2+1)^{\alpha+1}\Gamma(\alpha)} \int_0^\infty x^\alpha e^{-x} dx$$
$$= \frac{2r\beta\Gamma(\alpha+1)}{(\beta r^2+1)^{\alpha+1}\Gamma(\alpha)}. \quad (6)$$

B. Method of Fractional Moments

We now compute the moments of R, in order to be able to estimate the two unknown parameters α and β using the MoM similarly to [3]. From the definition of the moment, the nth order moment of R is

$$\mathrm{E}\{R^n\} = 2\alpha\beta \int_0^\infty \frac{r^{n+1}}{(\beta r^2+1)^{\alpha+1}} dr. \quad (7)$$

Substituting $k = \beta r^2$, and using the identities $B(z,w) = \int_0^\infty (t^{z-1}/(1+t)^{z+w}) dt = \Gamma(z)\Gamma(w)/\Gamma(z+w)$ and $\Gamma(\alpha+1) = \alpha\Gamma(\alpha)$, we have the closed form

$$\mathrm{E}\{R^n\} = \left(\frac{1}{\beta}\right)^{n/2} \alpha \int_0^\infty \frac{k^{n/2}}{(k+1)^{\alpha+1}} dk$$
$$= \left(\frac{1}{\beta}\right)^{n/2} \frac{\Gamma(n/2+1)\Gamma(\alpha-n/2)}{\Gamma(\alpha)} \quad (8)$$

which converges if and only if $\alpha > n/2$ [9].

The characteristic parameters of the texture, i.e., α and β (see (2)) can be estimated by equating the analytical expectations of two moments to their sample estimates given by the formula [3]:

$$\widehat{\mathrm{E}\{R^n\}} = \frac{1}{N_\mathrm{s}} \sum_{t=1}^{N_\mathrm{s}} |e(t)|^n \quad (9)$$

where $e(t)$ is the clutter sample and N_s is the number of samples. Recalling the constraint $\alpha > n/2$, for small values of α, estimation of $f_R(r)$ via the MoM may not be feasible for integer values of n, thus it is suggested [10] for small α to use the MoFM (i.e., to use value of n which are not necessarily integers). We have chosen to estimate these unknown parameters using the 1st and $\frac{1}{2}$th order moments as follows

$$\widehat{\mathrm{E}\{R\}} = \left(\frac{1}{\beta}\right)^{1/2} \frac{\Gamma(1+\frac{1}{2})\Gamma(\alpha-\frac{1}{2})}{\Gamma(\alpha)}$$
$$\widehat{\mathrm{E}\{R^{1/2}\}} = \left(\frac{1}{\beta}\right)^{1/4} \frac{\Gamma(1+\frac{1}{4})\Gamma(\alpha-\frac{1}{4})}{\Gamma(\alpha)}, \qquad \alpha > \tfrac{1}{2}. \quad (10)$$

C. Maximum Likelihood Estimation

We now estimate the unknown parameters α and β of the inverse gamma distributed clutter using the ML estimator [6]. From (6), the likelihood function of the data is given by the formula:

$$f_R(r;\alpha,\beta) = (2\alpha\beta)^{N_\mathrm{s}} \prod_{t=1}^{N_\mathrm{s}} \frac{r(t)}{(\beta r(t)^2+1)^{\alpha+1}}. \quad (11)$$

We can calculate the logarithm of this expression

$$\mathcal{L} = \log f_R(r;\alpha,\beta)$$
$$= N_\mathrm{s}\log(2\alpha\beta) - \sum_{t=1}^{N_\mathrm{s}} (\alpha+1)\log(\beta r(t)^2+1) + \text{const.} \quad (12)$$

In order to find the maximum of the likelihood function, we compute its partial derivatives with respect to α and β and let them equal to zero:

$$\frac{\partial\mathcal{L}}{\partial\alpha} = \frac{N_\mathrm{s}}{\alpha} - \sum_{t=1}^{N_\mathrm{s}} \log(\beta r(t)^2+1) = 0 \quad (13a)$$

$$\frac{\partial\mathcal{L}}{\partial\beta} = \frac{N_\mathrm{s}}{\beta} - (\alpha+1)\sum_{t=1}^{N_\mathrm{s}} \frac{r(t)^2}{\beta r(t)^2+1} = 0. \quad (13b)$$

From (13b) we can derive the expression of the ML estimate $\hat{\alpha}$ as a function of β,

$$\hat{\alpha}_\mathrm{ML} = \frac{N_\mathrm{s}}{\beta\sum_{t=1}^{N_\mathrm{s}} \frac{r(t)^2}{\beta r(t)^2+1}} - 1. \quad (14)$$

Substituting (14) into (13a), we obtain the concentrated log-likelihood function for β,

$$\mathcal{L}_\mathrm{c}(\beta) = \frac{N_\mathrm{s}\beta\sum_{t=1}^{N_\mathrm{s}} \frac{r(t)^2}{\beta r(t)^2+1}}{N_\mathrm{s} - \beta\sum_{t=1}^{N_\mathrm{s}} \frac{r(t)^2}{\beta r(t)^2+1}} - \sum_{t=1}^{N_\mathrm{s}} \log(\beta r(t)^2+1). \quad (15)$$

The ML estimate of β is a zero point of this function.

[1]The Rayleigh distribution is $f_{|x|}(\rho) = 2\rho e^{-\rho^2}$.

D. Cramér-Rao Bound

From the partial derivatives (13), we can compute the Fisher information matrix (FIM) [11]

$$I = \begin{pmatrix} \frac{N_s}{\alpha^2} & N_s \mathrm{E}\left\{\frac{R^2}{\beta R^2+1}\right\} \\ N_s \mathrm{E}\left\{\frac{R^2}{\beta R^2+1}\right\} & \frac{N_s}{\beta^2} - N_s(\alpha+1)\mathrm{E}\left\{\frac{R^4}{(\beta R^2+1)^2}\right\} \end{pmatrix}. \tag{16}$$

Note that the expectations in the FIM can be easily obtained by using the same procedure as (8). Then the variances for any unbiased estimator $\hat{\alpha}$ and $\hat{\beta}$ satisfy [11]

$$\mathrm{var}(\hat{\alpha}) \geq [I^{-1}(\alpha,\beta)]_{11} = \frac{N_s}{\beta^2 \det(I)} - \frac{N_s}{\det(I)}(\alpha+1)\mathrm{E}\left\{\frac{R^4}{(\beta R^2+1)^2}\right\} \tag{17a}$$

$$\mathrm{var}(\hat{\beta}) \geq [I^{-1}(\alpha,\beta)]_{22} = \frac{N_s}{\alpha^2 \det(I)} \tag{17b}$$

where

$$\det(I) = \frac{N_s^2}{\alpha^2\beta^2} - N_s^2 \frac{\alpha+1}{\alpha^2}\mathrm{E}\left\{\frac{R^4}{(\beta R^2+1)^2}\right\} - N_s^2 \mathrm{E}^2\left\{\frac{R^2}{\beta R^2+1}\right\}$$

is the determinant of matrix I.

IV. RESULTS

A. Numerical Examples

We present numerical examples to assess the accuracy of estimation by comparing the MSEs of the ML and MoFM estimates of α and β with their CRBs for the inverse gamma texture. Here the parameters were set to $\alpha = \beta = 1$. The sample MSE of the estimators were calculated using 4000 independent trials. Fig. 1 shows the CRBs and MSEs for both the ML and the MoFM estimates of α, as a function of the number of independent samples simulated N_s. Fig. 2 shows the MSEs and CRB for both the ML and the MoFM estimates of β, as a function of N_s. The ML estimate is asymptotically unbiased. We observe that the MSE of the ML estimator approaches the CRB when the number of observations increases, which means the ML estimations are also efficient. The MSE of the MoFM estimates does not attain the CRB when the observation number increases. However, it is interesting to observe that for small numbers of observation, the MoFM estimator of β (Fig. 2) has lower MSE than the CRB, implying that it is biased. For the computation complexity, since iteration methods (e.g., Newton-Raphson method) are often used to find the root of (15), MoFM takes less time than ML estimates.

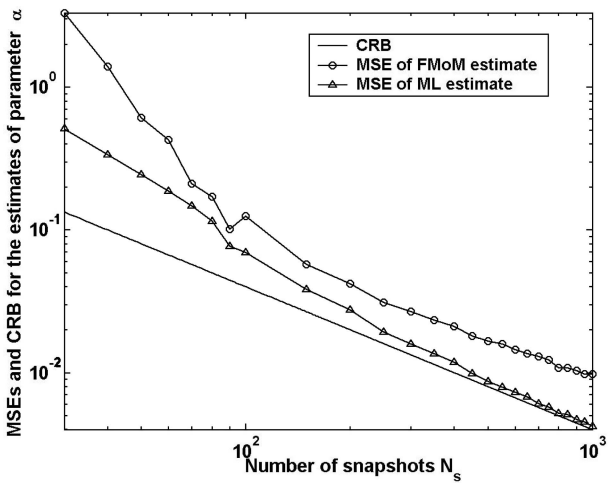

Fig. 1. MSEs and CRB versus number of snapshots for parameter α, ($\alpha = 1$, $\beta = 1$).

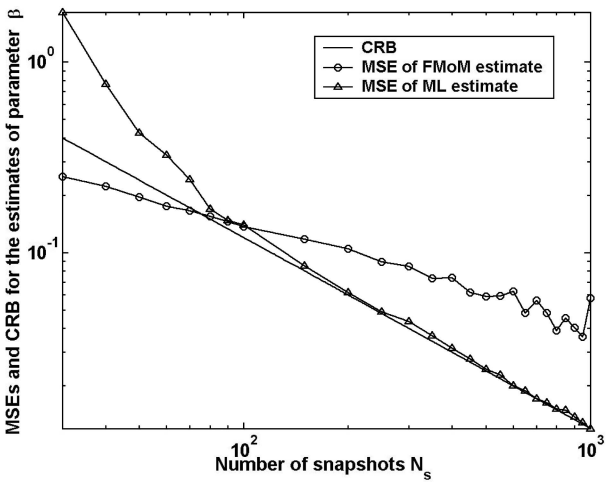

Fig. 2. MSEs and CRB versus number of snapshots for parameter β, ($\alpha = 1$, $\beta = 1$).

B. Real Data Analysis

We now demonstrate the application of the developed model to real lake-clutter data. The lake-clutter data we processed were collected at Grimsby, Ontario, with the McMaster University IPIX radar. IPIX is an experimental X-band search radar, capable of dual polarized and frequency agile operation. The characteristic features of the IPIX radar are summarized in [12] and Table I. The radar site was located at east of the "Place Polonaise" at Grimsby, Ontario (Latitude 43.2114°N, Longitude 79.5985°W), looking at lake Ontario from a height of 20 m. The nearest shore on the far side of the lake is more than 20 Km away. The data of the Grimsby database are stored in 222 files, as 10 bits integers. There are like polarizations, HH and VV (Lpol), and

TABLE I
Radar Characteristics

Transmitter	Receiver	Parabolic Dish Antenna
TWT peak power: 8 KW	Number of receivers: 2	Diameter: 2.4 m
Dual frequency transmission: 8.9–9.4 GHz	Outputs: Linear, I and Q	Pencil beam width (Azim. Res.) 1.1 deg
H and V polarization, agile	Receiving polariz. H-V	Antenna gain: 45.7 dB
Pulse width: 20 ns to 5000 ns (real) 5000 ns (expanded) 32 ns (compressed)	Data acquisition: Sample rate: 0 to 50 MHz Outputs: Linear, I, Q	Cross-pol. isolation: 30 dB
PRF: from 0 to 20 KHz	Quantization: 10 bit-up to 16 bit effective	Double pol. with central feeder

cross-polarizations, HV and VH (Xpol), coherent reception, leading to a quadruplet of I and Q values for Lpol and Xpol. In this work we show the results of our analysis on one file recorded on February 4, 1998 at about 10:30 pm. During the recordings the radar was transmitting with a pulse-repetition frequency (PRF) of 1000 Hz and a pulse length of 0.06 μs leading to a range resolution of 9 m. In order to investigate the statistical properties of the data, we compare the empirical pdf of the data with the developed analytical inverse gamma texture compound model and with log-normal (LN), Weibull (W), and K pdfs. The expression of these pdfs and their moments are reported below [2, 13].

Log Normal Model:

$$f_R(r) = \frac{1}{\sqrt{2\pi\sigma^2}} \exp\left(-\frac{1}{2\sigma^2}(\log r - \log\delta)^2\right) u(r) \tag{18}$$

$$\mathrm{E}\{R^n\} = \delta^n \exp(n^2\sigma^2/2) \tag{19}$$

where σ is the shape parameter and δ is the scale parameter.

Weibull Model:

$$f_R(r) = \frac{c}{b}\left(\frac{r}{b}\right)^{c-1} \exp(-(r/b)^c) u(r) \tag{20}$$

$$\mathrm{E}\{R^n\} = b^n \Gamma\left(\frac{n}{c+1}\right) \tag{21}$$

where c is the shape parameter and b is the scale parameter.

K Model:

$$f_R(r) = \frac{\sqrt{4\nu/\mu}}{2^{\nu-1}\Gamma(\nu)} \left(\sqrt{\frac{4\nu}{\mu}} r\right)^{\nu} K_{\nu-1}\left(\sqrt{\frac{4\nu}{\mu}} r\right) u(r) \tag{22}$$

$$\mathrm{E}\{R^n\} = \left(\frac{\mu}{\nu}\right)^{n/2} \frac{\Gamma(\nu + n/2b)\Gamma(n/2+1)}{\Gamma(\nu)} \tag{23}$$

where $\Gamma(\cdot)$ is the Gamma function, $K_{\nu-1}$ is the modified Bessel function of the third kind of order $\nu - 1$, ν is the shape parameter and μ is the scale parameter.

The parameter of log-normal (LN), Weibull (W), and K pdfs have been estimated by the classical MoM, by equating the first and second experimental and theoretical moments as in [3] and [13].

We estimate the parameters of the analytical inverse gamma distribution using both the MoFM and ML estimator, as presented in Section III. Considering correlated clutter is beyond the scope of this paper. Table II reports these estimates of the parameters for cell 9 of the data set 19980204-224024-ANTSTEP for VV, HH, and VH polarized data. This estimates have been computed by using N_s = 60,000 samples. The clutter to noise ratio (CNR) has been estimated to be about 20 dB for all the polarizations, thus the thermal noise can be neglected [3, Sect. 2.3]. The results of the histogram analysis for the VV, HH, and VH data in cell 9 are reported in Fig. 3, Fig. 4 and Fig. 5, where we plot the clutter magnitude pdfs by substituting the estimated parameters into the theoretical clutter's magnitude pdfs and compare them with the histogram of real radar data. The results show a very good fit to the tail of VV and HH data with the inverse gamma compound-Gaussian model. The pdf of the ML method and the one from the MoFM do not show a significant deviation from each other. To measure the goodness of fit, we have evaluated the root mean-square error (RMSE) defined as in [14]–[15]

$$\mathrm{RMSE} = \frac{1}{N_P}\sum_{k=1}^{N_P} |p_R(k) - h(k)|^2$$

where $p_R(\cdot)$ is the generic pdf whose parameters are estimated from the real data, $h(\cdot)$ is the real data

TABLE II
Estimated Parameters, Grimsby Database, Cell 9

	Inverse Gamma MoFM			Inverse Gamma ML			W			LN			K		
Pol.	α	$\beta 10^3$	RMSE	α	$\beta 10^3$	RMSE	c	b	RMSE	σ	$\ln\delta$	RMSE	ν	$\mu 10^{-4}$	RMSE
VV	1.85	0.977	0.5250	1.8587	0.985	0.5422	1.2011	0.0284	2.7647	0.7281	−3.8876	2.0178	0.8263	6.0636	2.3817
HH	1.55	2.2696	1.4681	1.5582	2.3102	1.5217	1.0152	0.0205	5.7743	0.8235	−4.2326	2.7647	0.52	4.0893	5.6748
VH	1.5250	11.142	3.3010	1.4946	11.474	3.3128	1.1498	0.0098	9.4423	0.7520	−4.9571	4.04	0.7284	0.76639	7.8181

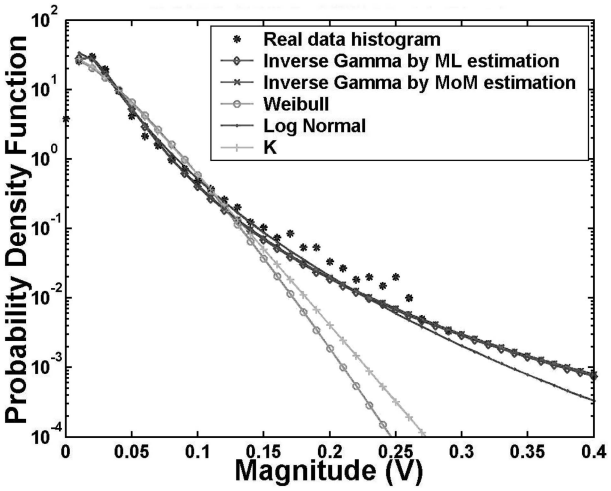

Fig. 3. Probability density functions of the clutter magnitude, VV polarization, 9th-range cell.

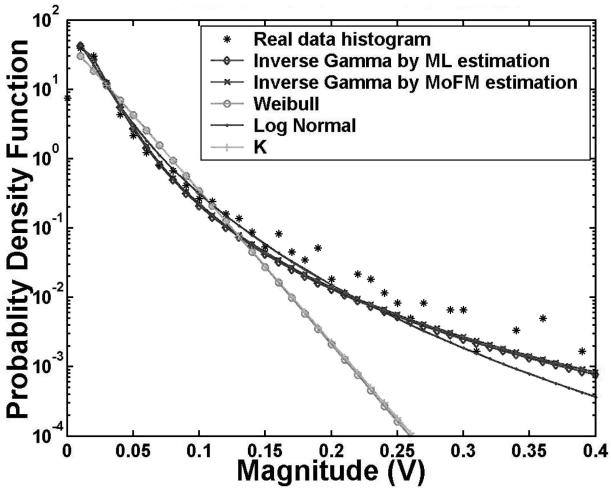

Fig. 4. Probability density functions of the clutter magnitude, HH polarization, 9th-range cell.

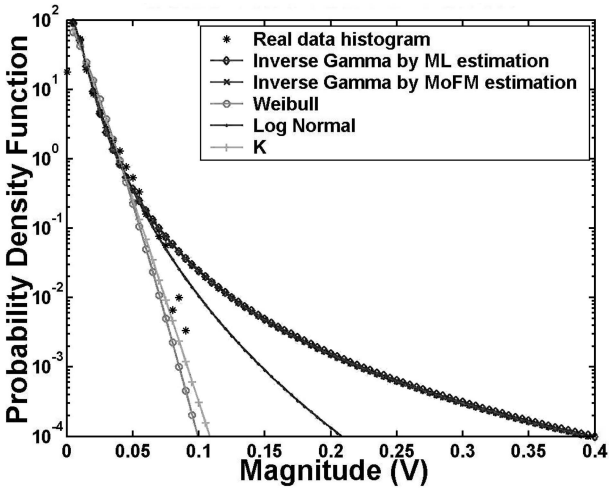

Fig. 5. Probability density functions of the clutter magnitude, VH polarization, 9th-range cell.

histogram, and k is the generic point of the amplitude axis in which both histogram and pdf are evaluated. We have found that the RMSEs for the inverse gamma compound-Gaussian model are the smallest, as evident in Table II, where we report the values of RMSE for each polarization and each model.

V. CONCLUSIONS

Compound-Gaussian models are useful for modeling the distribution of sea-clutter data. We have considered the use of inverse gamma distributed texture of this model due to the ease in estimating its parameters. We developed ML and MoFM estimates to find these parameters, and presented numerical examples to asses the accuracy of these estimations. One result has shown that, as expected, the ML estimates are asymptotically efficient. On the other hand, the mean-square errors of the MoFM estimates do not attain the CRB when the number of observations increases. We then performed a statistical analysis of real lake-clutter data amplitude. Our results showed that these data can be very well fitted to the inverse gamma distributed texture compound-Gaussian model. We focused our analysis on a range cell for VV, HH, and VH data. To explore the goodness of fit we evaluated the RMSEs. The results indicated that the inverse gamma texture model gives the least RMSE value. Considering that real sea-clutter data are often temporally correlated, the proposed ML will be extended by taking this correlation into account in our future work.

ACKNOWLEDGMENTS

The authors wish to express their gratitude to Dr. Eytan Paldi and Prof. Fulvio Gini for their helpful comments.

ALLESSIO BALLERI
Departimento di Ingegneria dell'Informazione
Università di Pisa
Via C. Caruso 14
56122 Pisa
Italy

ARYE NEHORAI[1]
JIAN WANG
Dept. of Electrical and Computer Engineering
University of Illinois at Chicago
851 S. Morgan St.
1120 SEO (M/C 154)
Chicago, IL 60607-7053
E-mail: (nehorai@ese.wust.edu)

[1]Current address: Dept. of Electrical and Systems Engineering, Washington University in St. Louis, Bryan Hall, Room 201, Campus Box 1127, One Brookings Dr., St. Louis, MO 63130.

REFERENCES

[1] Yao, K.
Spherically invariant random processes: Theory and applications.
In V. K. Bhargava, et al., (Eds.), *Communications, Information and Network Security*, Dordrecht, The Netherlands: Kluwer Academic Publishers, 2002, ch. 16, 315–332.

[2] Gini, F., Greco, M. V., Diani, M., and Verrazzani, L.
Performance analysis of two adaptive radar detectors against non-Gaussian real sea clutter data.
IEEE Transactions on Aerospace and Electronic Systems, **36** (Oct. 2000), 1429–1439.

[3] Farina, A., Gini, F., Greco, M. V., and Verrazzani, L.
High resolution sea clutter data: A statistical analysis of recorded live data.
IEE Proceedings, **144** (June 1997), 121–130.

[4] Conte, E., and Longo, M.
Characterisation of radar clutter as a spherically invariant random process.
IEE Proceedings, Pt. F, **134** (Apr. 1997), 191–197.

[5] Gini, F., and Greco, M.
Texture modelling, estimation and validation using measured sea clutter data.
Proceedings of the IEE, Radar, Sonar, Navigation, **149** (June 2002), 115–124.

[6] Dogandžić, A., Nehorai, A., and Wang, J.
Maximum likelihood estimation of compound-Gaussian clutter and target parameters.
In *Proceedings of 12th Annual Workshop Adaptive Sensor Array Processing* (ASAP '04), Lincoln Laboratory, Lexington, MA, Mar. 2004.

[7] Emmanuelle, J., Ovarlez, J. P., Declercq, D., and Duvaut, P.
BORD: Bayesian optimum radar detector.
Signal Processing, **83**, 6 (2003), 1151–1162.

[8] Lange, K. L., Little, R. J. A., and Taylor, J. M. G.
Robust statistical modeling using the t distribution.
Journal of the American Statistical Association, **84** (Dec. 1989), 881–896.

[9] Abramowitz, M., and Stegun, I. A. (Eds.)
Handbook of Mathematical Functions with Formulas, Graphs, and Mathematical Tables.
New York: Dover, 1972.

[10] Iskander, D. R., and Zoubir, A. M.
Estimation of the parameters of the K-distribution using higher order and fractional moments.
IEEE Transactions on Aerospace and Electronic Systems, **35** (Oct. 1999), 1453–1457.

[11] Kay, S. M.
Fundamental of Statistical Signal Processing: Esimation Theory.
Prentice Hall Signal Processing Series Alan V. Oppenheim, series editor, Englewood Cliffs, NJ: Prentice-Hall, 1993.

[12] Conte, E., De Maio, A., and Galdi, C.
Statistical analysis of real clutter at different range resolutions.
IEEE Transactions on Aerospace and Electronic Systems, **40**, 3 (July 2004).

[13] Greco, M., Gini, F., and Diani, M.
Robust CFAR detection of random signals in compound-Gaussian clutter plus thermal noise.
IEE Proceedings, Pt. F, **148** (Aug. 2001), 227–232.

[14] Griffiths, H. D.
Knowledge-based solutions as they apply to the general radar problem.
In *Proceedings of the Research Technology Organization*, North Atlantic Treaty Organization Lecture Series 233, Knowledge-Based Radar Signal and Data Processing, Rome, Italy, Nov. 6–7, 2000.

[15] Greco, M., Bordoni, F., and Gini, F.
X-band sea-clutter nonstationarity: Influence of long waves.
IEEE Journal of Oceanic Engineering, **29** (Apr. 2004), 269–283.

[16] Anastassopoulos, V., Lampropoulos, G. A., Drosopoulos, A., and Rey, N.
High resolution radar clutter statistics.
IEEE Transactions on Aerospace and Electronic Systems, **35** (Jan. 1999), 43–60.

Performance Analysis of Passive Low-Grazing-Angle Source Localization in Maritime Environments Using Vector Sensors

We consider the problem of passive estimation of source direction-of-arrival (DOA) and range using polarization-sensitive sensor arrays, when the receiver array and signal source are near the sea surface. The scenario of interest is the case of low-grazing-angle (LGA) propagation in maritime environments. We present a general polarimetric signal model that takes into account the interference of the direct field with the field reflected from smooth and rough surfaces. Using the Cramér-Rao bound (CRB) and mean-square angular error (MSAE) bound, we analyze the performance of different array configurations, which include an electromagnetic vector sensor (EMVS), a distributed electromagnetic component array (DEMCA), and a distributed electric dipole array (DEDA). By computing these bounds, we show significant advantages in using the proposed diversely polarized arrays compared with the conventional scalar-sensor arrays.

I. INTRODUCTION

Tracking targets and radio sources flying near the sea surface is a problem of considerable relevance, mainly because conventional radar systems may experience low performance [1]. In this scenario, the signal arrives at the radar receiver via both a direct and an indirect path, the latter produced by reflections on the sea surface (multipath propagation). The two

Manuscript received May 2, 2005; revised June 5, 2006; released for publication December 18, 2006.

IEEE Log No. T-AES/43/2/903030.

Refereeing of this contribution was handled by E. S. Chornoboy.

This work was supported by the Department of Defense under the Air Force Office of Scientific Research MURI Grant FA9550-05-1-0443, AFOSR Grant FA9550-05-1-0018, and DARPA funding under NRL Grant N00173-06-1-G006.